pH Dependence on Colorimetric Detection of Hg^{2+} by Histidine-Functionalized Gold Nanoparticles

Dewi Eviane, Dwi Siswanta, and Sri Juari Santosa*

Department of Chemistry, Faculty of Mathematics and Natural Sciences, Universitas Gadjah Mada, Sekip Utara, Yogyakarta 55281, Indonesia

** Corresponding author:*

tel: +62-8164262984
email: sjuari@ugm.ac.id

Received: November 24, 2019
Accepted: January 20, 2020

DOI: 10.22146/ijc.51824

Abstract: *In this study, we successfully developed gold nanoparticles capped with histidine (His-AuNPs) for Hg^{2+} detection using trisodium citrate as the reducing agent. The optimum pH for the detection of Hg^{2+} by His-AuNPs was 12. The addition of Hg^{2+} to the His-AuNPs caused the color change from red to black-blue, which is readily detectable by the naked eye. This color change is followed by a decrease in the intensity of the primary Surface Plasmon Resonance (SPR) peak at a wavelength (λ) of 525 nm and an increase in the secondary peak at λ = 650 nm. His-AuNPs effectively detected Hg^{2+} with limits of detection and quantitation of 1.77 μM and 5.89 μM, respectively. His-AuNPs exhibited good performance for the detection of Hg^{2+} in waste water collected from a steel industrial facility in Banten Province, with a recovery and a percent relative standard deviation of 115% and 1.02%, respectively.*

Keywords: *AuNPs; histidine; Hg^{2+} detection; synthesis*

■ INTRODUCTION

Mercury is a heavy metal that frequently contaminates the environment. Natural environmental mercury is mainly the result of volcanic activity; however, human activities also contribute to the increasing levels of mercury through metal mining, forest fires, solid-waste incineration, and the combustion of fossil fuels (coal, oil, and gas) [1-2]. The divalent mercury ion (Hg^{2+}) is the most common form of mercury and is stable when dissolved in water [3]; this mercury species binds easily to amino acids in the body. Mercury is difficult to decompose biologically and persists in ecosystems. The health effects of mercury include damage to the nervous system, heart, kidneys, and bone [4].

Hg^{2+} has usually been analyzed by atomic adsorption spectroscopy (AAS), inductively coupled plasma optical emission spectroscopy (ICP-OES) and mass spectrometry (ICP-MS), high-performance liquid chromatography (HPLC), advanced mercury analysis (AMA), and gas chromatography-atomic fluorescence spectroscopy (GC-AFS) [5-7]. The previous methods are mostly time consuming and require a laboratory. One alternative method that is fast and simple is colorimetric detection using gold nanoparticles (AuNPs). Colorimetric detection is based on interactions between a target compound and the surfaces of AuNPs, which results in a visually distinct color change.

The major advantage of the use of AuNPs is the ability to functionalize their surfaces with a variety of functional groups. Functional groups on the AuNP surfaces not only stabilize the AuNPs in solution but also provide sites for interactions with metal ions through coordination [8]. The interactions between the functional groups of capping agents and metals affect AuNP stability, which can lead to AuNP aggregation [9]. Aggregation increases the sizes of AuNPs, which results in a red-to-blue color change; a shift and expansion of the surface plasmon resonance (SPR) are also observable by UV-Vis spectroscopy [10].

Various chemicals have been used as capping agents in the synthesis of nanoparticles for metal detection. 4,4-Dipyridine compounds have been used as capping agents in the synthesis of AuNPs for the detection of Hg^{2+} [11]. AuNPs stabilized Tween-20 were used as a probe for the colorimetric detection of Hg^{2+}

[12]. However, 4,4-dipyridine and Tween-20 were toxic compounds and not environmentally friendly. Amino acids have been used as capping agents because they were green and biocompatible [14]. The amino acid contains more than one functional group, namely carboxylic acid and amino groups; these functional groups can interact with more than one metal ion [11]. Several amino acids have been used as capping agents for synthesized AuNPs to detect metal ions. Sener et al. showed that AuNPs synthesized using 11-mercaptoundecanoic acid and five amino acids (lysine, cysteine, histidine, tyrosine, and arginine) as capping agents are capable of detecting some toxic heavy-metal ions [12]. In another publication, Sener et al. reported the syntheses of AuNPs for the detection of Hg^{2+} using trisodium citrate as the reducing agent and fourteen types of amino acids as capping agents [13]. Colorimetric detection was only observed when arginine and lysine were used as capping agents, whereas the use of histidine and the eleven other types of amino acids as capping agents did not alter the UV-Vis spectrum of the AuNPs. Liu et al. modified thymine in order to induced AuNPs aggregation in the presence of Hg^{2+} [14]. Chai et al. used l-cysteine-functionalized AuNPs to detect Hg^{2+} [15], while Liu et al. reported the use of AuNPs with cysteine capping agents for the detection of Cu^{2+} [11].

pH plays an important role in AuNP-based metal detection. Guan et al. successfully synthesized AuNPs for the detection of Fe^{3+} at a set pH with histidine as the capping agent [19], while Fu and co-workers adjusted the pH during the synthesis of AuNPs-glutathione for the detection of Ni^{2+} [20]. Inspired by this previous work, in this study, we adjusted the pH during the synthesis of AuNPs using trisodium citrate as the reducing agent and histidine as the capping agent in order to develop a system for the detection of Hg^{2+}. We expect that the developed system can be used to detect Hg^{2+} in wastewater samples.

■ EXPERIMENTAL SECTION

Materials

Solid gold with 99.99% purity was obtained from PT. ANTAM Indonesia. Analytical grade of trisodium citrate, histidine, HNO_3, $Hg(NO_3)_2$ and various standard solutions of $Cd(NO_3)_2$, $Zn(NO_3)_2$, $Cu(NO_3)_2$, $Cr(NO_3)_3$, $Pb(NO_3)_2$, $Fe(NO_3)_3$, $Co(NO_3)_2$, $Ag(NO_3)$, $Mg(NO_3)_2$, $Ni(NO_3)$, $Al(NO_3)$, $K(NO_3)$, $Na(NO_3)$, $Mn(NO_3)_2$ were used for this purpose. NaOH and HCl reagents were used to regulate pH. These compounds were obtained from Merck (Germany) and were used without further purification.

Instrumentation

The UV-Vis absorbance spectra were measured using Shimadzu UV-1700 PharmaSpec. The morphologies of the nanoparticles were characterized by Transmission Electron microscopy (TEM, JEOL JEM-1400). The nanoparticles size and zeta potential were determined by Particle Size Analysis (PSA) Horiba SZ-100. The infrared spectra were analyzed by Fourier Transform Infrared (FTIR) using a Shimadzu FTIR Prestige-21. The crystal structures of the nanoparticles were characterized by Shimadzu XRD-6000.

Procedure

Preparation of histidine functionalized AuNPs

Chloroauric acid ($HAuCl_4$) solution was prepared from 1 g certified gold metal 99.99% which was dissolved in 40 mL of aqua regia. Deionized water was added to increase the volume of the solution to 100 mL. AuNPs were synthesized by the widely used Turkevich method with a few modifications [18]. AuNPs were prepared in a test tube by adding 5 mL of 0.26 mM chloroauric acid solution to 5 mL of 0.02 M sodium citrate solution. The test tube was then placed and heated in a water bath at 95 °C for approximately 15 min. The solution color changed from clear yellow to dark red indicating the formation of AuNPs. To functionalized AuNPs with histidine, 5 mL of 0.1 mM histidine with a pH value of 1 to 13 was added to the synthesized AuNPs solution. The pH of the histidine solution was adjusted using a solution of 0.1 M NaOH and 0.1 M HCl.

Effect of reaction time

The effect of reaction time was determined by reacting 1 mL of the His-AuNPs with 1 mL of a 10 μM Hg^{2+} solution, and the absorbance of the resulting solution was measured using UV-Vis spectrophotometer at 10 min intervals for 120 min.

Detection of Hg^{2+}

The 1 mL solution of synthesized His-AuNPs was used as the colorimetric detection. The color change from red to purple to blue-black occurred after the addition of 1 mL of various Hg^{2+} concentrations. Colorimetric detection was carried out on industrial wastewater from Banten Province. Hg^{2+} concentration in wastewater was measured using a mercury analyzer. The collected samples were known to have Hg^{2+} concentrations of 3.55 nM. The samples were spiked with Hg^{2+} standard solution to become 3 and 5 μM. The color changes were observed using a UV-Vis spectrophotometer.

Effect of other cations

The effects of some other ions were investigated by the addition of Cd^{2+}, Zn^{2+}, Cu^{2+}, Cr^{3+}, Pb^{2+}, Fe^{3+}, Co^{2+}, Ag^{+}, Mg^{2+}, Ni^{2+}, Al^{3+}, K^{+}, Na^{+}, Mn^{2+}. Interference experiments were carried out by adding 0.5 mL of a 10 μM metal solution of the other metal ions to 0.5 mL of 10 μM Hg^{2+}, then was added to a 1 mL solution of the synthesized His-AuNPs. Colorimetric changes were observed using a UV-Vis spectrophotometer at wavelength 525 nm. A blank solution devoid of any additional metal cation was also tested.

Characterization

The SPR spectra were acquired at room temperature using a UV-Vis spectrophotometer directly after synthesis using a 1 cm optical path length quartz cuvette and 200–800 nm wavelength range. The morphologies of the AuNPs were characterized by Transmission Electron microscopy (TEM, JEOL JEM-1400). AuNPs for TEM analysis were prepared by immersing the copper grid into AuNPs solution then drying at room temperature. AuNPs size was determined by Particle Size Analysis (PSA, Horiba SZ-100). The zeta potential of the AuNPs solution was assessed using a Horiba SZ-100 Zeta Potential Analyzer. The Particle size and zeta potential were directly measured after synthesis using a 1 cm optical path length cuvette. The crystallinity of AuNPs achieved was investigated by Shimadzu XRD 6000. The interaction between AuNPs, reducing agent, capping agent, and Hg^{2+} was analyzed by FTIR. The sample was prepared by collecting nanoparticle deposits from the centrifugation of the nanoparticle solution.

■ RESULTS AND DISCUSSION

Effect of Histidine on SPR Peak of AuNPs

pH value is one of the most important factors that influenced the AuNPs system. One of the systems influenced is the SPR peak intensity of AuNPs [20]. In this study, the acidity of histidine solution was affected by the pK_a of histidine; based on its pK_a (α-NH_3^+: pK_a = 9.2, imidazole group or R: pK_a = 6.0, α-COOH: pK_a = 1.8) [19], His-AuNPs should be more stable under relatively alkaline conditions (pH 8–12). Under these conditions, all of the carboxyl and amino groups in the histidine capping agent are deprotonated, resulting in a negative potential zeta value of -64.4 mV (Table 1). This charge is due to the interactions between the AuNP surfaces and the carboxyl and amino groups of histidine that result in electrostatic repulsion. Fig. 1 shows SPR peak intensity of AuNPs synthesized using trisodium citrate as reducing agent and histidine as capping agent. Fig. 1(a) demonstrates that the addition of histidine at concentrations between 1 μM and 10 mM does not significantly influence the intensity of SPR peak at 525 nm. The addition of 0.1 mM histidine resulted in an increase in SPR peak intensity, but the SPR peak did not shift from 525 nm. His-AuNPs was less stable when the histidine solution was acidic (Fig. 1(b)), as evidenced by a decrease in the SPR peak intensity at 525 nm. Likewise, the His-AuNPs stability was also lower at very alkaline pH, as confirmed by the expanding SPR peak to a higher wavelength (red shift).

Effect of Histidine pH on the Detection of Hg^{2+}

Protein probes are strongly influenced by pH [21]. Histidine was added to the AuNPs under a variety of pH in order to ascertain the best conditions for the detection of Hg^{2+}. The histidine at the acidic solution is not completely deprotonated; hence interactions between the carboxylate and amine of His-AuNPs and Hg^{2+} were not optimal. All of the amine and carboxyl groups from histidine were deprotonated at pH 13; however, the possible reaction between OH^- in histidine solution at pH 13 and Hg^{2+} resulted in fewer interactions between His-AuNPs and Hg^{2+}.

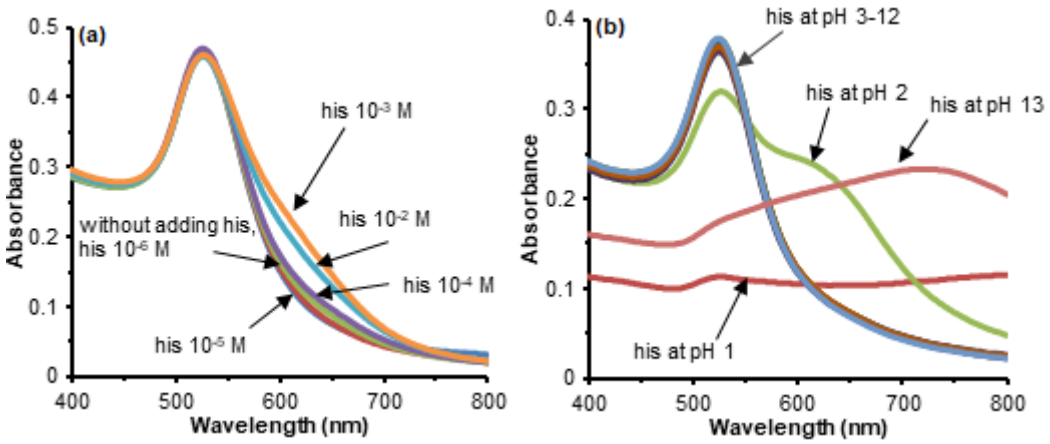

Fig 1. UV-vis spectra of (a) AuNPs with various concentrations of histidine, (b) His-AuNPs prepared with histidine at various acidity

Histidine solution at pH 12 was mixed with AuNPs and was added to Hg^{2+} solution to give a decrease in the intensity of the SPR peak at 525 nm and an appearance of new SPR peak at 650 nm. This corresponds to a red to blue-black color change when the sample was observed with the naked eye as seen in Fig. 2. These results were in line with the previous studies that a specific pH of cysteine as a capping agent could influence the formation of the SPR peak of AuNPs for the detection of glutathione colorimetry [22]. Li et al. reported that cysteine solutions with pH 5.8 affect AuNPs aggregation, resulting in changes in color and changes in SPR peak intensity.

Effect of Interaction Time on the Reaction of His-AuNPs and Hg^{2+}

The reaction time greatly affects the interactions between the His-AuNPs and Hg^{2+}, as shown in Fig. 3(a). The SPR intensity of His-AuNPs at 525 nm was measured every 5 min after the addition of 5 μM Hg^{2+} revealing the decrease in the intensity of SPR peak during the observation period to 100 min. The results show that the SPR intensity was stable after 100 min, indicating that the colorimetric detection was optimum after 100 min. Fig. 3(b) reveals that the decrease in the SPR intensity of His-AuNPs-Hg at 525 nm with increasing reaction time 0–120 min is due to red shifting, which indicates that the aggregation of His-AuNPs-Hg in the colloidal solution occurred. Furthermore, the addition of Hg^{2+} to His-AuNPs resulted in a new SPR peak at 650 nm, which was red-shifted to 700 nm with increasing reaction time. This observation is consistent with the formation of the larger size of nanoparticles through aggregation. This was confirmed by PSA that the His-AuNPs-Hg particles were larger than those of His-AuNPs (Table 1).

Colorimetric Detection Mechanism

Prior to the addition of Hg^{2+} ions, the AuNP and His-AuNPs solutions were red in color when viewed by the naked eye. The addition of Hg^{2+} to His-AuNPs resulted in a red to blue-black color change, which occurred within a few seconds after the addition of Hg^{2+} indicating a decrease in nanoparticle stability. This change was confirmed by UV-Vis spectroscopy, which revealed a decrease in the intensity of the original SPR

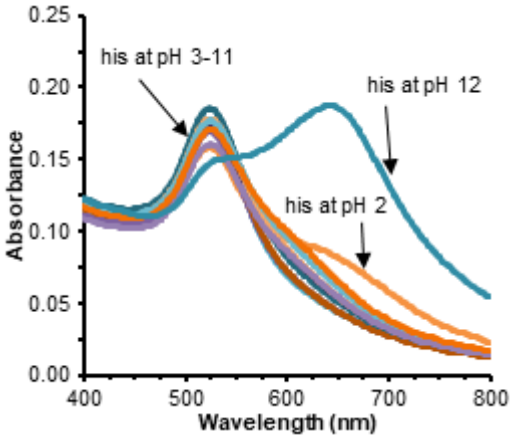

Fig 2. UV-Vis spectra of His-AuNPs with histidine prepared at various pH and added Hg^{2+}

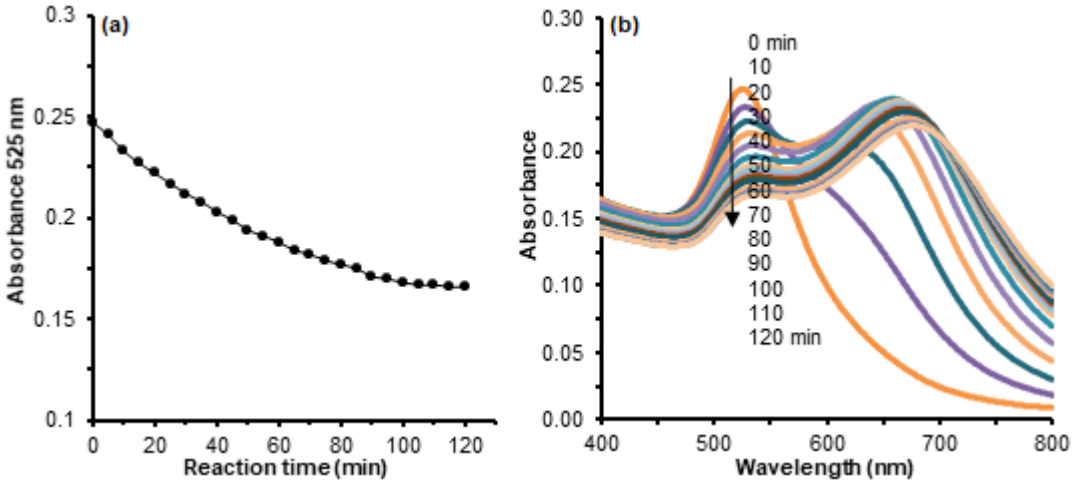

Fig 3. (a) The effect of reaction time between His-AuNPs and Hg^{2+} on the SPR peak at 525 nm. (b) The wavelength (400–800 nm) as a function of reaction time

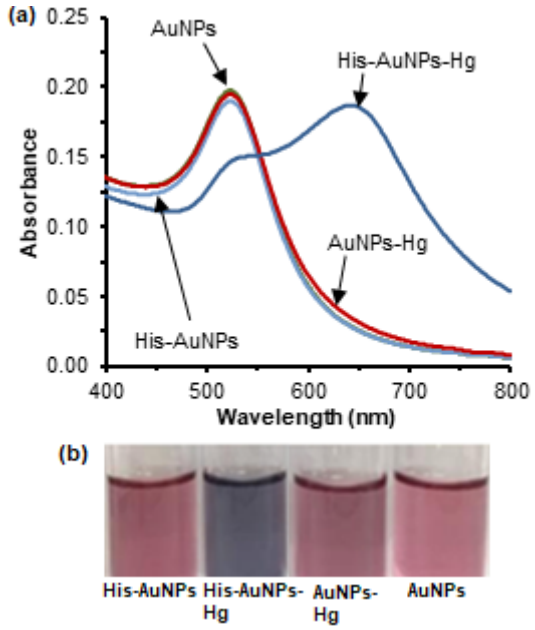

Fig 4. Colorimetric responses: (a) Spectra SPR of AuNPs, His-AuNPs, AuNPs-Hg, and His-AuNPs-Hg (b) picture of AuNPs, His-AuNPs, AuNPs-Hg, and His-AuNPs-Hg

peak at 525 nm and the formation of a new SPR peak above 650 nm (Fig. 4); this new SPR peak is ascribable to His-AuNPs aggregation. In addition, nanoparticles aggregation caused color changing and SPR peak widening [23]. This result is consistent with other studies that using AuNPs with thymine as a capping agent which showed the formation of new SPR peak UV-Vis spectra at around 650 nm after Hg^{2+} addition [20]. The color change of AuNPs colloid could be seen in Fig. 4(b).

Sener et al. predicted that aggregation between Hg^{2+} and lysine/arginine occurs because these two amino acids have two remaining amino group molecules that can interact with more than one Hg^{2+} to form bridges between particles [13]. Du et al. synthesized AuNPs using thymine as capping agents for colorimetric sensors of Hg^{2+} based on thymine coordination chemistry, resulting in aggregation of AuNPs [20]. Based on the report, we concluded that the mechanism for this colorimetric response was involving one amino group of histidine that is used to interact with AuNPs surface and two remaining amino groups belonging to histidine are used to provide a strong coordination interaction with Hg^{2+}. Fig. 5 showed the illustration of colorimetric sensors that occur between His-AuNPs and Hg^{2+} was based on histidine coordination chemistry.

Zeta Potential Analysis

Zeta Potential was determined at optimum conditions and room temperature. Zeta potential was measured by adding 5 mL of various Hg^{2+} concentrations to 5 mL His-AuNPs. The zeta potential is a surface-charge parameter of colloidal particles [24]. Colloidal particles with zeta potential values of more than +30 mV or less than -30mV are stable colloids due to strong electrostatic repulsion between particles thereby preventing aggregation [25]. The zeta potential

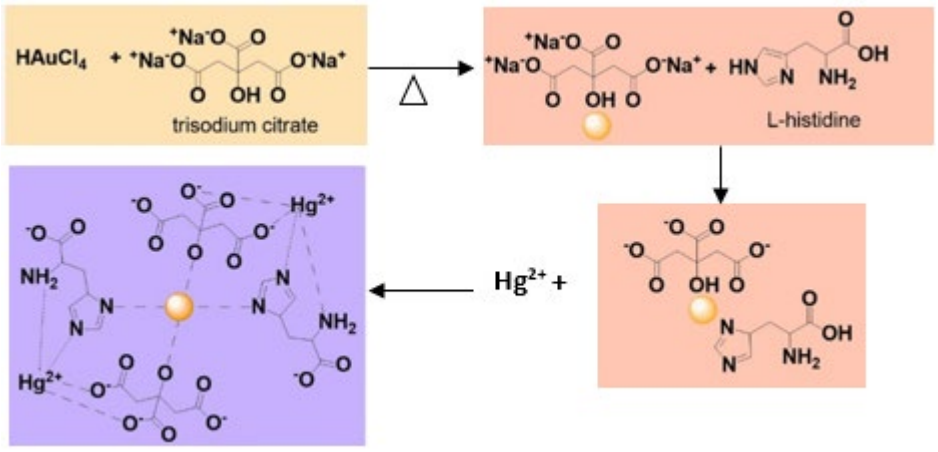

Fig 5. Schematic illustration Hg^{2+} detection by His-AuNPs

was used to indicate if the interactions between Hg^{2+} and His-AuNPs exist. The synthesized AuNPs have negative surface charges (Table 1), and the zeta potential of His-AuNPs was found to be more negative than that of the AuNPs, which indicates that the AuNPs solution is more stable after the addition of histidine. Interactions between the amino groups and the AuNP surface can result in a more-negative zeta potential of the colloid [26]. In our study, the existence of deprotonated amine and carboxylate from histidine that are on the surface of AuNPs will increase electrostatic repulsion, thereby increasing stability. Meanwhile, the addition of Hg^{2+} to His-AuNPs reduced the stability promoting an aggregation as indicated by the nanoparticle zeta potential being closer to zero. This means that the addition of Hg^{2+} to His-AuNPs affects the zeta potential. The higher the concentration of Hg^{2+} added, the closer the zeta potential of the His-AuNPs-Hg solution to zero. The stability of AuNPs after the addition of histidine and Hg^{2+} was confirmed with the observation of the particle size. Addition of histidine to AuNPs resulted in a decrease in the size of His-AuNPs, while addition of Hg^{2+} caused aggregation of His-AuNPs followed by increased size of His-AuNPs. The size of the nanoparticles was confirmed by PSA as shown in Table 1.

Effect of Other Cations to the Hg^{2+} Detection

Our work tested fourteen other cations (K^+, Co^{2+}, Na^+, Ag^+, Cu^{2+}, Mg^{2+}, Zn^{2+}, Mn^{2+}, Al^{3+}, Fe^{3+}, Cr^{3+}, Ni^{2+}, Pb^{2+}, and Cd^{2+}) to determine the effect of the other cations to the colorimetric Hg^{2+} detection. Fig. 6(a) shows that the SPR intensity at 525 nm only decreased with the addition of Hg^{2+}. The addition of fourteen other cations to His-AuNPs did not significantly reduce the SPR intensity at 525 nm. However, the addition of Ag^+ resulted in a slight increase of the SPR intensity of AuNPs since Ag^+ is stabilized by citrate [27]. Interference experiments were carried out by adding 0.5 mL of a 5 μM one of 14 cations to 0.5 mL of a 5 μM Hg^{2+}. The mixture of two cations was added to the 1 mL His-AuNPs. The addition

Table 1. Zeta potential and particle size of AuNPs, His-AuNPs and His-AuNPs-Hg

Sample	Zeta Potential (mV)	PSA (nm)
AuNPs	-34.8	Monodisperse 38.6
His-AuNPs	-64.4	Monodisperse 32.1
His-AuNPs-Hg 5 μM	-11.5	Monodisperse 252.8
His-AuNPs-Hg 7 μM	-10	
His-AuNPs-Hg 9 μM	-6.3	
His-AuNPs-Hg 11 μM	-2.1	

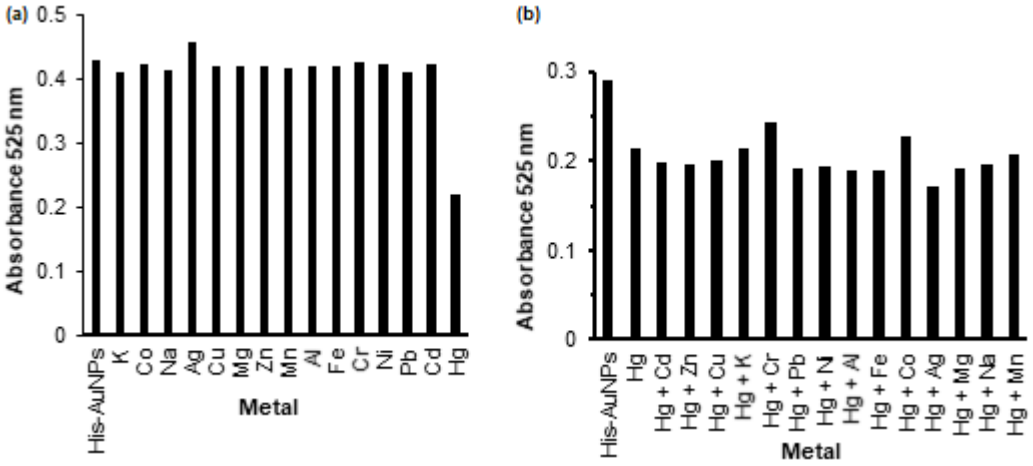

Fig 6. SPR intensity of His-AuNPs in the presence of (a) one cation (b) two cations (Hg^{2+} with one other cation) on 525 nm

of other cations to the Hg^{2+} had essentially no effect on the His-AuNPs detection-response to Hg^{2+}. A visual color change from red to blue-black was noted and was confirmed by UV-Vis spectroscopy (Fig. 6(b)).

Detection of Hg^{2+}

In this work, we have successfully synthesized His-AuNPs using trisodium citrate as a reducing agent and histidine as a capping agent for Hg^{2+} detection. Hg^{2+} at different concentrations were tested to determine the sensitivity of the colorimetric-detection method, and the change in the absorbance at 525 nm (ΔA_{525}) was plotted as a function of Hg^{2+} concentration (Fig. 7). Linearity determination was done by adding 5 mL Hg^{2+} to 5 mL His-AuNPs. ΔA_{525} was found to be linearly related to Hg^{2+} in the 9–16 µM concentration range (R = 0.909), with the limit of detection (LoD) and limit of quantitation (LoQ) for Hg^{2+} of 1.77 µM and 5.89 µM, respectively. The LoD was calculated by the equation LoD = 3 S_0/K and LoQ = 10 S_0/K, where S_0 was the standard deviation of the blank (n = 7) and K was the slope of the calibration line. The lowest detectable Hg^{2+} concentration in this work was 1.77 µM, which is above the allowed Hg^{2+} concentration limit (15.43 nM) in the environment defined by the Indonesian government (Indonesian Government Regulation number 82/2001). This assay could be used to determine mercury in the environment in accordance with the LOD and linearity range. Table 2 showed the comparison of the present method with the other reported values.

His-AuNPs was used to detect Hg^{2+} in real wastewater samples collected from an industrial site in Banten Province. Wastewater was filtered to remove any solids before testing. The concentration of Hg^{2+} in collected wastewater was 3.55 nM tested by using mercury analyzer. A recovery testing was performed by

Table 2. Performance of some typical colorimetric methods for the detection of Hg^{2+}.

Methods	Linear range	LOD	Ref
Colorimetric Lysine-AuNPs	1–60 nM	10 nM	[13]
Colorimetric Histidine-AuNPs	-	-	[13]
Colorimetric Thymine derivative-AuNPs	50-250 nM	0.8 nM	[20]
Colorimetric Cysteamine-AuNPs	0.05–3 µM	30 µM	[28]
Colorimetric Thioctic acid-AuNPs	0.01–1 µM	10 µM	[29]
Colorimetric Polyethyleneimine-AuNPs	0.003–5 µM	1.72 nM	[30]
Colorimetric 8-hydroxyquinolines and oxalates-AuNPs	10 nM to 100 mM	10 nM	[31]
Colorimetric Histidine-AuNPs	9–16 µM	1.77 µM	This work

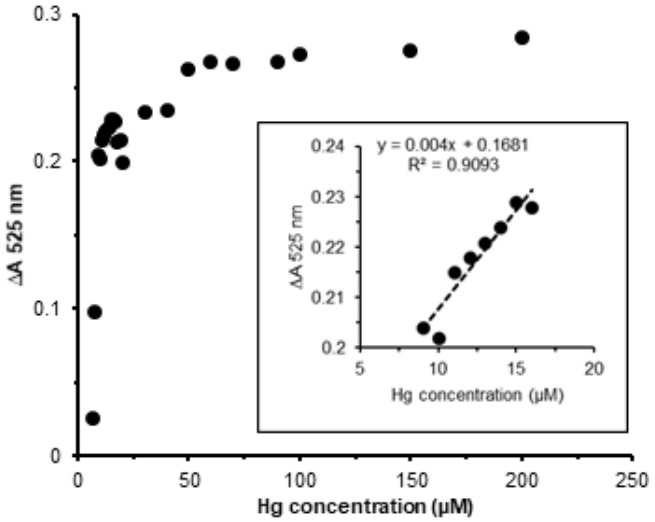

Fig 7. Response (ΔA525) of the colorimetric assay against increasing Hg^{2+} concentrations

spiking to concentrations of 3 and 5 μM, with the recovery value determined to be 115 ± 2% (n = 3). Repeatedly measuring the concentration of the 10 μM Hg^{2+} sample resulted in a percent relative standard deviation (%RSD) of 1.02%. These experimental results confirm the effectiveness of this detection method for quantifying Hg^{2+} in the waste water.

Characterization of AuNPs

The addition of a capping agent to the AuNPs affects both the particle size and distribution. The AuNPs exhibited a non-uniform nanoparticle size distribution with an average size of 38.6 nm with 82.9% of the nanoparticles were smaller than 100 nm and had monodispersed spherical morphologies. AuNPs with various sizes can be obtained when synthesized using the citrate reduction method, depending on the reactant molar ratio [26,32]. The size distribution of AuNPs was confirmed using PSA measurement (Fig. 8(a)) to give 97.5% of the nanoparticles smaller than 100 nm with an average size of 32.1 nm (Fig. 8(b)). The spherical morphologies of these nanoparticles were also characterized by TEM. Fig. 9(a) shows TEM images of AuNPs synthesized using trisodium citrate as the reducing

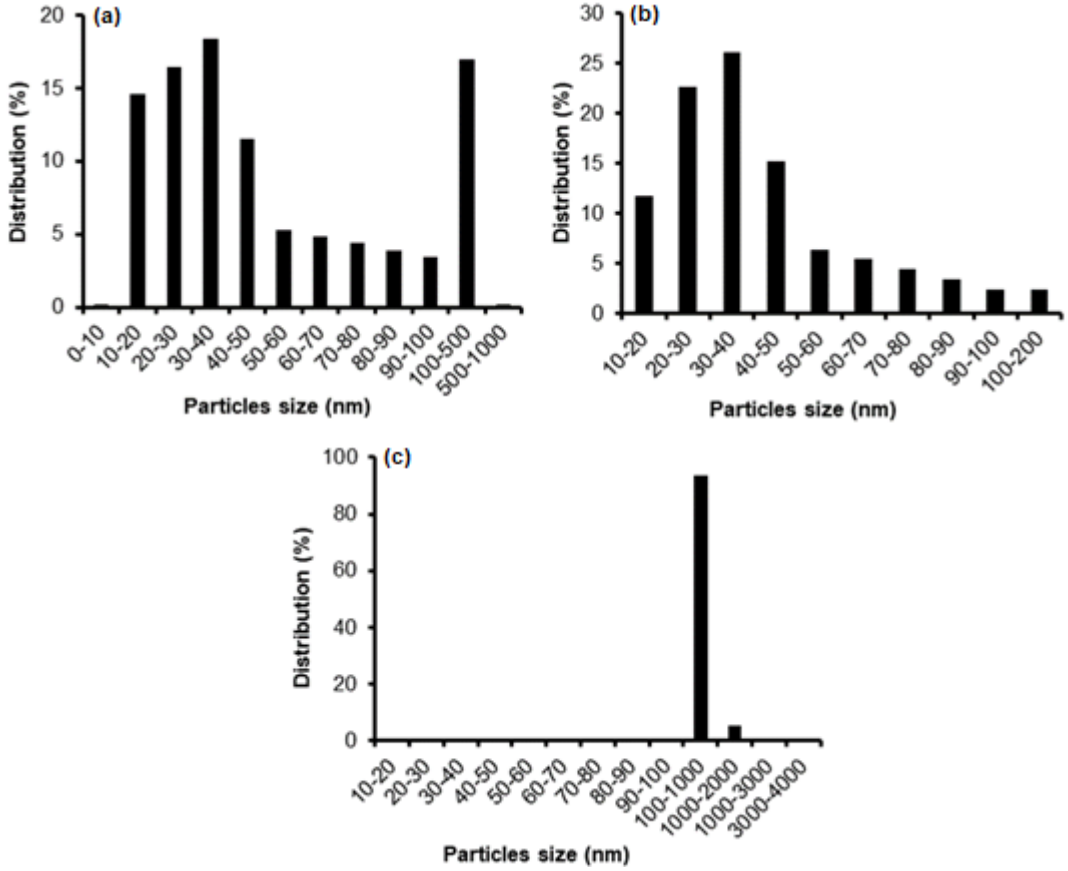

Fig 8. Particle-size distributions of (a) AuNPs (b) His-AuNPs, and (c) His-AuNPs-Hg

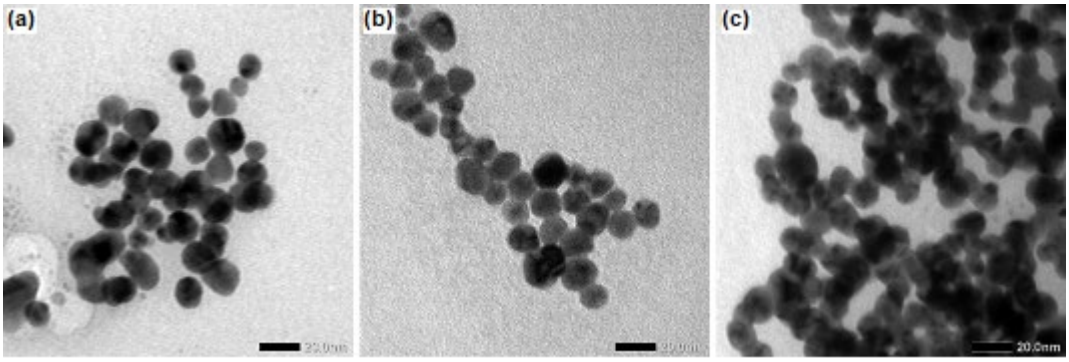

Fig 9. TEM images of (a) AuNPs, (b) His-AuNPs, and (c) His-AuNPs-Hg

agent. The addition of histidine to the AuNPs resulted in smaller and relatively uniformly distributed nanoparticles (Fig. 9(b)). We conclude that the addition of histidine as a stabilizing agent affects nanoparticle size. Fig. 9(c) shows that the addition of 10 μM Hg^{2+} resulted in larger nanoparticles due to aggregation. The average size of the His-AuNPs particles after the addition of Hg^{2+} was 252.8 nm.

Characterization using FTIR showed the differences between AuNPs before and after the addition of histidine and Hg^{2+} as shown in (Fig. 10). The AuNPs FTIR spectra showed OH stretching bands around 3448 cm^{-1} and OH bending at 1635 cm^{-1}. The C-O vibration band is shown at 1381 cm^{-1}. The C=O band was found at wavelengths 1651 and 1558 cm^{-1}. The characteristic band of AuNPs shows the functional group on trisodium citrate around Au(0). His-AuNPs FTIR spectra show bands around the wave number 3448 cm^{-1} which are sharper than AuNPs because of the stretching contribution of -NH. The interaction of AuNPs with histidine causes the vibration of band stretching C=O to shift from 1651 and 1658 cm^{-1} to 1627 and 1573 cm^{-1}, and the sharpening of the C-O peak at the wavenumber 1381 cm^{-1}. FTIR spectra changes were evident that His-AuNPs interact with Hg^{2+}. The His-AuNPs-Hg spectra showed a reduction in the band at a wavelength of 3448 cm^{-1} which was possible because of the interaction of the amine group on His-AuNPs with Hg^{2+}. The interaction of his-AuNPs with Hg^{2+} causes vibration band stretching of C=O at wavelengths of 1627 cm^{-1} experienced a shift to 1589 cm^{-1}.

XRD measurement was conducted to determine the phase composition and crystal structure of AuNPs. Peaks from AuNPs and His-AuNPs reveal the formation of gold nanoparticles due to diffraction (111), (200), (220), (311), and (222) with face centered cubic crystal shapes (fcc) (Fig. 11). XRD AuNPs and His-AuNPs patterns are consistent with the results of previous studies [19,33]. The XRD pattern between AuNPs and His-AuNPs has a

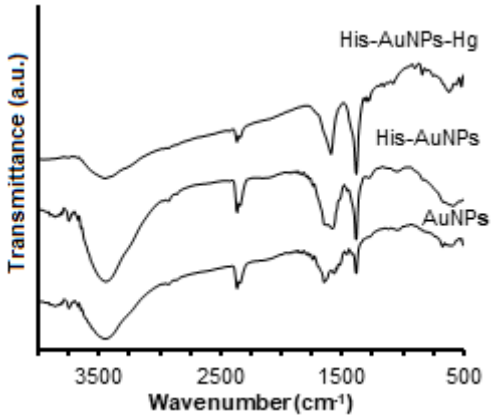

Fig 10. FTIR spectra of AuNPs, His-AuNPs, and His-AuNPs-Hg

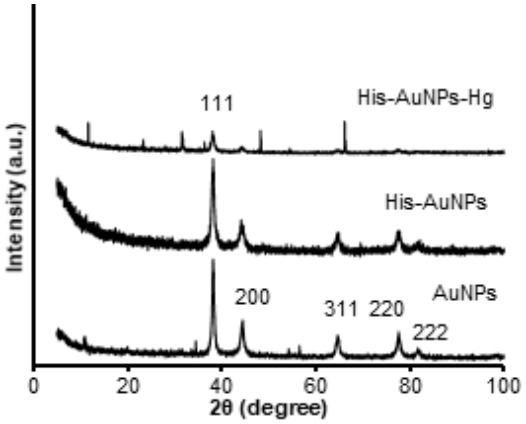

Fig 11. XRD patterns of the AuNPs, His-AuNPs, and His-AuNPs-Hg

similar crystallinity according to their intensity. These results are based on the reference of the Joint Committee on Powder Diffraction Standard (JCPDS 04-0784), which suggests that the crystalline gold nanoparticles were formed. However, the addition of Hg^{2+} causes a decrease in peak intensity in the XRD diffraction pattern (111), (200), (220), (311), which is probably due to the aggregation of nanoparticles as evidenced in the TEM image. This result is in line with Tripathy et al. which reported that the aggregation of AuNPs due to the addition of Fe^{3+} caused a decrease in the peak XRD intensity characteristic of AuNPs [34].

■ CONCLUSION

In this study, colorimetric detection of Hg^{2+} using His-AuNPs has successfully been done by adjusting the pH of the histidine solution that significantly affected the aggregation of His-AuNPs. UV-Vis spectroscopy revealed that the addition of Hg^{2+} to His-AuNPs resulted in a decrease in absorbance at 525 nm only when histidine solution at pH 12 was used, with new peaks observed at wavelengths of around 650 nm. The change in color from red to blue-black was readily observed with the naked eye. This mercury detection method showed a good selectivity with limits of detection and quantitation for Hg^{2+} of 1.77 µM and 5.89 µM, respectively.

■ REFERENCES

[1] Apilux, A., Siangproh, W., Praphairaksit, N., and Chailapakul, O., 2012, Simple and rapid colorimetric detection of Hg(II) by a paper-based device using silver nanoplates, *Talanta*, 97, 388–394.

[2] Brasca, R., Onaindia, M.C., Goicoechea, H.C., de la Peña, A.M., and Culzoni, M.J., 2016, Highly selective and ultrasensitive turn-on luminescence chemosensor for mercury(II) determination based on the rhodamine 6G derivative FC1 and Au nanoparticles, *Sensors*, 16 (10), 1652.

[3] Du, J., Liu, M., Lou, X., Zhao, T., Wang, Z., Xue, Y., Zhao, J., and Xu, Y., 2012, Highly sensitive and selective chip-based fluorescent sensor for mercuric ion: Development and comparison of turn-on and turn-off systems, *Anal. Chem.*, 84 (18), 8060–8066.

[4] Miretzky, P., and Cirelli, A.F., 2009, Hg(II) removal from water by chitosan and chitosan derivatives: A review, *J. Hazard. Mater.*, 167 (1-3), 10–23.

[5] Xie, Z.J., Bao, X.Y., and Peng, C.F., 2018, Highly sensitive and selective colorimetric detection of methylmercury based on DNA functionalized gold nanoparticles, *Sensors*, 18 (8), 2679.

[6] Suvarapu, L.N., and Baek, S.O., 2017, Recent studies on the speciation and determination of mercury in different environmental matrices using various analytical techniques, *Int. J. Anal. Chem.*, 2017, 3624015.

[7] Azemard, S., and Vassileva, E., 2015, Determination of methyl mercury in marine biota samples with advanced mercury analyzer: Method validation, *Food Chem.*, 176, 367–375.

[8] Oliveira, E., Núñez, C., Santos, H.M., Fernández-Lodeiro, J., Fernández-Lodeiro, A., Capelo, J.L., and Lodeiro, C., 2015, Revisiting the use of gold and silver functionalised nanoparticles as colorimetric and fluorometric chemosensors for metal ions, *Sens. Actuators, B*, 212, 297–328.

[9] Lou, T., Wang, Y., Li, J., Peng, H., Xiong, H., and Chen, L., 2011, Rapid detection of melamine with 4-mercaptopyridine-modified gold nanoparticles by surface-enhanced Raman scattering, *Anal. Bioanal. Chem.*, 401, 333–338.

[10] Priyadarshini, E., and Pradhan, N., 2017, Chemical gold nanoparticles as efficient sensors in colorimetric detection of toxic metal ions: A review, *Sens. Actuators, B*, 238, 888–902.

[11] Liu, J.M., Wang, H.F., and Yan, X.P., 2011, A gold nanorod based colorimetric probe for the rapid and selective detection of Cu^{2+} ions, *Analyst*, 136 (19), 3904–3910.

[12] Sener, G., Uzun, L., and Denizli, A., 2014, Colorimetric sensor array based on gold nanoparticles and amino acids for identification of toxic metal ions in water, *ACS Appl. Mater. Interfaces*, 6 (21), 18395–18400.

[13] Sener, G., Uzun, L., and Denizli, A., 2014, Lysine-promoted colorimetric response of gold nanoparticles: A simple assay for ultrasensitive

mercury(II) detection, *Anal. Chem.*, 86 (1), 514–520.

[14] Liu, X., Cheng, X., Bing, T., Fang, C., and Shangguan, D., 2010, Visual detection of Hg^{2+} with high selectivity using thymine modified gold nanoparticles, *Anal. Sci.*, 26 (11), 1169–1172.

[15] Chai, F., Wang, C., Wang, T., Ma, Z., and Su, Z., 2009, L-cysteine functionalized gold nanoparticles for the colorimetric detection of Hg^{2+} induced by ultraviolet light, *Nanotechnology*, 21 (2), 025501.

[16] Guan, J., Jiang, L., Li, J., and Yang, W., 2008, pH-dependent aggregation of histidine-functionalized Au nanoparticles induced by Fe^{3+} ions, *J. Phys. Chem. C*, 112, 3267–3271.

[17] Fu, R., Li, J., and Yang, W., 2012, Aggregation of glutathione-functionalized Au nanoparticles induced by Ni^{2+} ions, *J. Nanopart. Res.*, 14, 929.

[18] Turkevich, J., Stevenson, P.C., and Hiller, J., 1951, A study of the nucleation and growth processes in the synthesis of colloidal gold, *Discuss. Faraday Soc.*, 11, 55–75.

[19] Liu, Z., Zu, Y., Fu, Y., Meng, R., Guo, S., Xing, Z., and Tan, S., 2010, Hydrothermal synthesis of histidine-functionalized single-crystalline gold nanoparticles and their pH-dependent UV absorption characteristic, *Colloids Surf., B*, 76 (1), 311–316.

[20] Du, J., Wang, Z., Fan, J., and Peng, X., 2015, Chemical gold nanoparticle-based colorimetric detection of mercury ion via coordination chemistry, *Sens. Actuators, B*, 212, 481–486.

[21] Poornima, V., Alexandar, V., Iswariya, S., Perumal, P.T., and Uma, T.S., 2016, Gold nanoparticle-based nanosystems for the colorimetric detection of Hg^{2+} ion contamination in the environment, *RSC Adv.*, 6 (52), 46711–46722.

[22] Li, J.F., Huang, P.C., and Wu, F.Y., 2017, Specific pH effect for selective colorimetric assay of glutathione using anti-aggregation of label-free gold nanoparticles, *RSC Adv.*, 7, 13426–13432.

[23] Annur, S., Santosa, S.J., Aprilita, N.H., Phuong, N.T., and Phuoc, N.V., 2018, Rapid Synthesis of Gold Nanoparticles without Heating Process, *Asian J. Chem.*, 30 (11), 2399–2403.

[24] Bhattacharjee, S., 2016, DLS, and zeta potential – What they are and what they are not ?, *J. Controlled Release*, 235, 337–351.

[25] Yoosaf, K., Ipe, B.I., Suresh, C.H., and Thomas, K.G., 2007, In situ synthesis of metal nanoparticles and selective naked-eye detection of lead ions from aqueous media, *J. Phys. Chem. C*, 111 (34), 12839–12847.

[26] Zakaria, H.M., Shah, A., Konieczny, M., Hoffmann, J.A., Nijdam, A.J., and Reeves, M.E., 2013, Small molecule- and amino acid-induced aggregation of gold nanoparticles, *Langmuir*, 29 (25), 7661–7673.

[27] Wang, G.L., Zhu, X.Y., Jiao, H.J., Dong, Y.M., and Li, Z.J., 2012, Ultrasensitive and dual functional colorimetric sensors for mercury(II) ions and hydrogen peroxide based on catalytic reduction property of silver nanoparticles, *Biosens. Bioelectron.*, 31 (1), 337–342.

[28] Ma, Y., Jiang, L., Mei, Y., Song, R., Tian, D., and Huang, H., 2013, Colorimetric sensing strategy for mercury(II) and melamine utilizing cysteamine-modified gold nanoparticles, *Analyst*, 138 (18), 5338–5343.

[29] Su, D., Yang, X., Xia, Q., Chai, F., Wang, C., and Qu, F., 2013, Colorimetric detection of Hg^{2+} using thioctic acid functionalized gold nanoparticles, *RSC Adv.*, 3 (46), 24618–24624.

[30] Kim, K.M., Nam, Y.S., Lee, Y., and Lee, K.B., 2018, A highly sensitive and selective colorimetric Hg^{2+} ion probe using gold nanoparticles functionalized with polyethyleneimine, *J. Anal. Methods Chem.*, 2018, 1206913.

[31] Gao, Y., Li, X., Li, Y., Li, T., Zhao, Y., and Wu, A., 2014, A simple visual and highly selective colorimetric detection of Hg^{2+} based on gold nanoparticles modified by 8-hydroxyquinolines and oxalates, *Chem. Commun.*, 50 (49), 6447–6450.

[32] Kumar, S., Gandhi, K.S., and Kumar, R., 2007, Modeling of formation of gold nanoparticles by citrate method, *Ind. Eng. Chem. Res.*, 46 (10), 3128–3136.

[33] Halder, A., Das, S., Bera, T., and Mukherjee, A.,

2017, Rapid synthesis for monodispersed gold nanoparticles in kaempferol and anti-leishmanial efficacy against wild and drug resistant strains, *RSC Adv.*, 7 (23), 14159–14167.

[34] Tripathy, S.K., Woo, J.Y., and Han, C.S., 2013, Colorimetric detection of Fe(III) ions using label-free gold nanoparticles and acidic thiourea mixture, *Sens. Actuators, B*, 181, 114–118.